Heliyon 10 (2024) e38672

Contents lists available at ScienceDirect

Heliyon

journal homepage: www.cell.com/heliyon

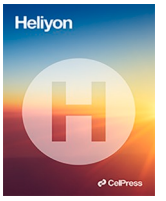

Research article

Polyglycerol Sebacate/polycaprolactone/reduced graphene oxide composite scaffold for myocardial tissue engineering

Azadeh Rejali [a], Mehdi Ebrahimian-Hosseinabadi [a,*], Anousheh Zargar Kharazi [b]

[a] Department of Biomedical Engineering, Faculty of Engineering, University of Isfahan, Isfahan, Iran
[b] Department of Biomaterials, Nano Technology and Tissue Engineering, School of Advanced Technologies in Medicine, Isfahan University of Medical Sciences, Isfahan, Iran

ARTICLE INFO

Keywords:
Myocardial tissue engineering
Scaffold
Polyglycerol sebacate
Polycaprolactone
Reduced graphene oxide

ABSTRACT

The aim of this research was to fabricate and evaluate polyglycerol sebacate/polycaprolactone/reduced graphene oxide (PGS-PCL-RGO) composite scaffolds for myocardial tissue engineering. Polyglycerol sebacate polymer was synthesized using glycerol and sebacic acid prepolymers, confirmed by Fourier-transform infrared spectroscopy (FTIR) and X-ray diffraction (XRD). Six PGS-PCL-RGO composite scaffolds (S_1-S_6) with various weight ratios were prepared in chloroform (CF) and acetone (Ace) solvents at 8 CF:2Ace and 9 CF:1Ace volume ratios, using the electrospinning method at a rate of 1 ml/h and a voltage of 18 kV. The scaffolds' chemical composition and microstructure were characterized by FTIR, XRD, and scanning electron microscopy (SEM). Further investigations included tensile testing, contact angle testing, four-point probe testing for electrical conductivity, degradation testing, and cytotoxicity testing (MTT). The results showed that adding 2%wt RGO to the composite scaffold decreased fiber diameter and degradation rate, while increasing electrical conductivity and ductility. The 33%PGS-65%PCL-2%RGO (S_3) composite scaffold exhibited the lowest degradation rate (23.87 % over 60 days) and the highest electrical conductivity (51E-3 S/m). Mechanical evaluations revealed an elastic modulus of 2.46 MPa and elongation of 62.43 %, aligning closely with the heart muscle's elastomeric properties. The contact angle test indicated that the scaffold was hydrophilic, with a water contact angle of 61 ± 2°. Additionally, the cell toxicity test confirmed that scaffolds containing RGO were non-toxic and supported good cell viability. In conclusion, the 33%PGS-65%PCL-2%RGO composite scaffold exhibits mechanical and structural properties similar to heart tissue, making it an ideal candidate for myocardial tissue engineering.

1. Introduction

According to published statistics, cardiovascular diseases (CVDs) are one of the most important causes of death in the world, with 17.3 million deaths per year. Based on these statistics, estimates suggest that by 2030, it will reach about 23.6 million deaths per year, which is about 31 % of the total annual deaths in the world [1]. The etiology of tissue damage in the cardiovascular system mainly includes damage caused by atherosclerosis and tissue ischemia such as myocardial infarction, degenerative diseases, and cardiomyopathies. The human heart is a complex organ that consists of various types of cells such as cardiomyocytes (CM), fibroblasts,

* Corresponding author. Department of Biomedical Engineering, Faculty of Engineering, University of Isfahan, Azadi Sq., Isfahan 81746, Iran.
E-mail address: m.ebrahimian@eng.ui.ac.ir (M. Ebrahimian-Hosseinabadi).

https://doi.org/10.1016/j.heliyon.2024.e38672
Received 4 July 2024; Received in revised form 26 September 2024; Accepted 27 September 2024
Available online 27 September 2024

endothelial cells, valvular interstitial cells, and cardiac stem cells. Cardiac cells are metabolically very active; they need adenosine triphosphate (ATP) for their physiological function. However, the heart lacks endogenous repair or regeneration potential. Any defect in cardiomyocyte size or deficiency in number leads to MI-related cardiovascular complications [2,3]. A heart attack or myocardial infarction and related electrical disturbances occur when the blood vessels that supply blood to the heart become blocked, leading to insufficient blood reaching a part of the heart, causing the cells in that area to die due to lack of nourishment [4]. A heart attack is often accompanied by abnormalities in the electrical function of the cardiovascular system, which are known as arrhythmias, and followed by failure. In this arrhythmia, the lack of electrical current conduction as well as non-directional conduction leads to the lack of electrical coupling at the level of connections between cells. As a result, despite the ability of the implanted cell to repair heart attack, the lack of functional coupling donor cells with host tissue can prevent electrical communication between them. In most cardiovascular disorders, including heart attack, collagen scar tissue, which acts as an insulator for electrical conduction, is created in the heart tissue. The collagen scar tissue insulates part of the heart muscle fibers and reduces the conduction of the path; it also reduces the action potential and ultimately causes an irregular heartbeat [5]. At present, the common methods of reducing cardiovascular diseases, including heart attack, by drug treatments and other clinical measures, have effectively improved the patient's survival and quality of life after tissue damage [2]. However, this is only a short-term solution. The permanent treatment will be through surgery and heart transplantation, but the issue that is always raised in this field is the severe shortage of donor organs, complications after transplantation, and the limited effectiveness of drug interventions on cell scaffold-based treatment approaches for cardiovascular diseases (CVDs). Due to the importance of the electrical conductivity of the heart to restore the contractility of cardiac muscle cells and heart function, innovative methods such as heart tissue engineering based on biomaterials have emerged recently. The advent of cardiac tissue engineering (CTE) has not only provided significant hope to resolve or salvage the damaged heart after MI but also provides a permanent treatment for the regeneration of the damaged myocardium [2].

One of the challenges in tissue engineering is choosing the right biomaterial for medical applications. Various biomaterials such as metals, polymers, ceramics, and composites are used in heart tissue engineering. In the meantime, polymers are chosen as suitable biomaterials due to their processability, reasonable cost, the availability of materials with desirable physical and mechanical properties, the ability to add reinforcing particles to them as a polymer matrix composite, and the potential for surface treatment. Due to flexibility and control of biodegradability, synthetic polymers usually have great advantages over natural polymers making them one of the most important biomaterials for medical applications. In recent years, research activity has increased in the development and clinical application of degradable elastomers as transplantable biological materials for soft tissue engineering, including heart tissue [6]. Polyglycerol sebacate (PGS) is one of the polymers widely used in soft tissue engineering, including the heart. PGS is the result of the synthesis of glycerol and sebacic acid, both of which are FDA-approved for medical use. Glycerol (a three-factor alcohol) and sebacic acid (a two-factor acid) during a condensation reaction, in vacuum pressure and high temperature, convert to PGS [7]. This polymer is hydrophilic and biodegradable, and its by-products are naturally metabolized in the body. It has been reported that the degradation time of polyglycerol sebacate in the body is about 60 days [8]. It also has mechanical properties close to heart muscle tissue. Polyglycerol sebacate has a Young's modulus of 0.04–1.2 MPa and a tensile strength of 0.20–0.5 MPa, and its most important feature is that it is an elastomer to imitate the heart muscle. The results of Differential Scanning Calorimetry (DSC) showed that this polymer is completely amorphous at a temperature of 37 °C [8]. In research, it was reported that PGS has been widely investigated for tissue engineering applications due to its elastomeric properties and biocompatibility [7]. The combination of PGS and polycaprolactone (PCL) can be considered in heart tissue engineering and its applications. PCL is a degradable and hydrophobic polyester aliphatic approved by the Food and Drug Administration (FDA) for use in the human body. PCL has a melting temperature of 59–64 °C and a glass transition temperature of −60 °C. Also, the modulus of this polymer is 343.9–364.3 MPa, tensile strength is 10.5–16.1 MPa [8]. The advantages of this polymer include its biological degradation, its compatibility with a wide range of other polymers, and its good processability, which allows the construction of various structures and shapes. Also pointed out the ease of melt processing due to its high thermal stability and relatively low cost [9]. Therefore, to control the PGS scaffold degradation rate and improve the manufacturing process, including the electrospinning method, PCL is added to produce porous scaffolds suitable for heart tissue engineering. In a study, it was investigated that the versatility of PGS-PCL scaffolds with the bioactive function of vascular endothelial growth factor (VEGF) along with their good sutureability can be used as a matrix with potential mechanical support permeable to damaged myocardium for cardiac tissue engineering [10]. Heart tissue is a dense, regular, and non-convergent structure, which includes cardiomyocytes and supporting cells [11]. To create coordination and continuity of the function of contraction and relaxation of the heart muscle tissue, the stimulating and conducting components must interact with the active cardiomyocytes to ultimately lead to the improvement of one-way blood flow with appropriate pressure [12]. Graphene and its derivatives are among the materials that have recently been considered in heart tissue engineering [13]. The synthesis of reduced graphene oxide (RGO) due to the reduction of graphene oxide (GO) improves the thermal conductivity, and when used together with polymers, it makes them conductive. It is common to add chemical-reducing agents to GO solutions, these can include hydrazine, metal hydrides, or hydraulic acids. RGO can also be synthesized through photocatalyzed reactions. In recent years, it has been reported that several "green" reducing agents such as ascorbic acid, sugars, amino acids, and even microorganisms are effective in RGO synthesis. These agents have advantages in scalability, energy consumption, and the amount of produced chemical waste [14]. Therefore, RGO can be added to the composite scaffold due to its good electrical conductivity to improve the electrical conductivity. By increasing the C/O ratio in the RGO structure, also losing oxygen-containing compounds, this material becomes hydrophobic, which can lead to the control of the degradation process and balance in the level of hydrophilicity of the scaffolds. In a study, it was reported that the injection of RGO together with Mesenchymal stem cells (MSCs) for the treatment of heart muscle infarction in mice resulted in positive results; the addition of RGO due to its electrical conductivity and the ability to absorb ECM proteins led to an increase in the expression Angiogenic growth factors and connexin-43 were found in MSCs. The injection of MSC-RGO into the infarcted area of rat heart muscle increased the repair of

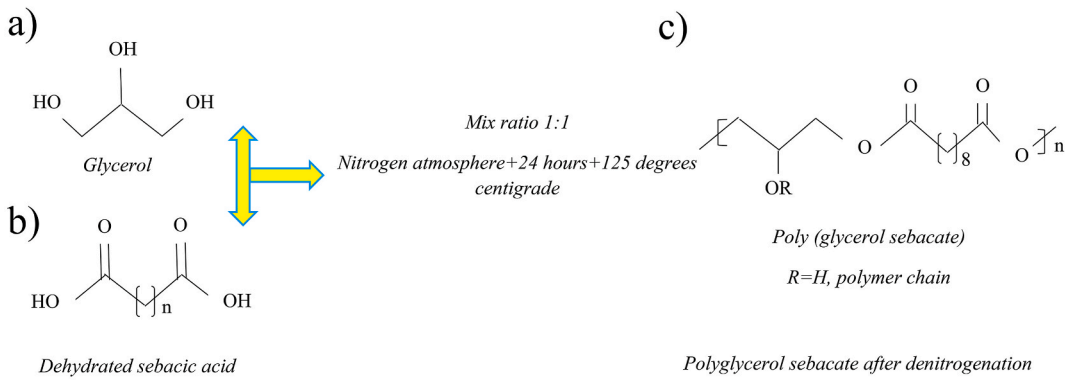

Fig. 1. The synthesis of polyglycerol sebacate involves a) the glycerol formula, b) the formula for dehydrated sebacic acid, and c) the chemical formula of the synthesized polyglycerol sebacate.

Table 1
Chemical composition and solvent ratios of electrospun scaffolds.

Sample	% PGS	% PCL	%RGO	CF:Ace (v/v%)
S_1	33	67	0	8:2
S_2	33	66	1	9:1
S_3	33	65	2	9:1
S_4	50	50	0	8:2
S_5	49	50	1	9:1
S_6	48	50	2	9:1
S_7	0	100	0	8:2

heart tissue and improved cardiac function compared to the injection of RGO or MSCs alone into this area [15]. In another study, the physicochemical and biological effects of increasing the concentration of reduced graphene oxide coating on the collagen scaffold and its antibacterial properties were investigated. The results indicate that increasing the RGO coating with a certain concentration can improve the mechanical properties and cell viability of cardiomyocytes by increasing the expression of heart genes. Recently, the antibacterial activity of RGO has been proven against *Escherichia coli* and *Staphylococcus aureus* for various tissue engineering applications [16].

In this research, polyglycerol sebacate/polycaprolactone/reduced graphene oxide (PGS-PCL-RGO) composites with different weight percentages were prepared, and composite scaffolds were fabricated by the electrospinning method. The chemical, mechanical, electrical, and biological properties of these scaffolds were evaluated for the use of myocardial tissue engineering to introduce the best composite scaffold for use in this field.

2. Materials and methods

2.1. Materials

Sebacic acid (>98 %), Glycerol (>99 %), Chloroform (CF) (>99 %), and Acetone were purchased from Merck (Germany). Polycaprolactone ($\bar{M}n$ = 80000 g/mol), MTT (3-(4,5-dimethylthiazol-2-yl)-2,5-diphenyltetrazolium bromide), and isopropanol were supplied by Sigma-Aldrich (USA). Reduced graphene oxide (RGO) powders with a purity higher than 95 % and plates below 10 layers with a thickness of 2 μm were supplied by Yazd Nano Sanjesh (Iran). PBS (Phosphate-buffered saline), FBS (Fetal bovine serum), and DMEM (Dulbecco's Modified Eagle Medium) were supplied by Bioidea (Iran). Finally, HUVECs (Human umbilical vein endothelial cells, NCBI code: C554) were purchased from the Pasteur Institute cell bank (Iran). All chemical components were used without further purification and were used as received.

2.2. Fabrication of PGS-PCL and PGS-PCL-RGO composite scaffolds

First, the synthesis of polyglycerol sebacate was considered. For this purpose, two substances, glycerol, and sebacic acid, approved by the American Food and Drug Administration (FDA) for medical applications, were used. Fig. 1 shows the synthesis steps of PGS; after preparing glycerol (Fig. 1a) and dehydrating sebacic acid (with a 1:1 ratio) (Fig. 1b), these two substances were placed in an oil bath under a nitrogen atmosphere at a temperature of 125 °C and mixed. After preparation, the sample was placed in a vacuum oven with a temperature of 40 °C and a pressure of 200 mTorr for 24 h, leading to the formation of the PGS polymer (Fig. 1c).

After the synthesis of polyglycerol sebacate, the fabrication of various scaffolds was considered. Table 1 shows the chemical

formulations and ratios of solvents of electrospun composite scaffolds. In this research, two compounds with weight ratios of (1:1) 50 % PGS-50 % PCL and (1:2) 33 % PGS-67 % PCL polyglycerol sebacate to polycaprolactone and four compounds with the same compositions with 1 % wt and 2 % wt of reduced graphene oxide (RGO) 33 % PGS-66 % PCL-1% RGO, 33 % PGS-65 % PCL-2% RGO, 49 % PGS-50 % PCL-1% RGO, 48 % PGS-50 % PCL-2% RGO were prepared in chloroform (CF) and acetone (Ace) solvents with 8 CF:2Ace (for samples without RGO) and 9 CF:1Ace (for samples with RGO) volume ratios.

First, the weight of polyglycerol sebacate and polycaprolactone polymers was calculated according to the desired weight percentages; then it was dissolved in chloroform solvent at ambient temperature using a magnetic stirrer at 1250 rpm. After that, reduced graphene oxide particles, according to the chemical formulation, were weighed and dispersed in chloroform solvent using an ultrasonic probe for 10 min. Then the solution containing polyglycerol sebacate and polycaprolactone was added to the solution containing reduced graphene oxide and placed on the stirrer at 1500 rpm for 30 min to obtain a uniform solution. After that, acetone was added to the final solution in the 8 CF:2Ace and 9 CF:1Ace volume ratios, for samples without RGO and with RGO, respectively, to increase the electrical conductivity of the solution and lead to the improvement of the electrospinning process [17]. The samples with RGO are more conductive compared to the samples without RGO. Therefore, the Ace volume ratio was selected to be lower than others. For scaffold fabrication, the electrospinning method was used; an electrospinning machine that included a high-voltage power source, a syringe pump for injecting the prepared solution in a 1 ml syringe, and a circular collector (drum) with a rotation of 200 rpm was used to produce fibers. Electrospinning was performed at room temperature with a voltage of 18 kV and a flow rate of 1 ml/h with a distance of 17 cm from the tip of the needle to the collector. The aluminum plate containing the electrospun fibers was dried at room temperature for 24 h, and the fibers were separated from the surface.

2.3. Characterization of composite scaffolds

To characterize and determine the functional groups of synthesized polyglycerol sebacate and electrospun scaffolds, a Jasco 6300 model FT-IR analyzer (Japan) was used. The scan was carried out over the range of 400–4000 cm^{-1}. X-ray diffraction patterns of electrospun scaffolds were obtained using the X′-pert model XRD analysis machine (Netherlands), with the 2θ angle ranging from 5 to 80°. SEM was employed for morphological investigations, electrospun fiber diameter measurements, and determination of porosity percentage of prepared scaffolds (n = 20). Before imaging, the samples were coated with a thin layer of gold and evaluated with a Philips XL 30 model SEM equipment (Netherlands).

The hydrophilicity of the scaffolds was evaluated using the contact angle measurement technique, following ASTM D-5946 standard, utilizing a contact angle analyzer (CA-ES10) manufactured in Iran. A volume of 4 μL of distilled water was placed on the samples to create a droplet. The device automatically measured the right and left angles of the droplet, and images of the droplet shape were recorded within 5 s. Subsequently, the contact angle between the drop and the scaffold was measured at 5 points on its surface for each group of samples by analyzing the recorded images [18,19].

The biodegradability of electrospun composite scaffolds was evaluated in vitro according to ASTM F-1635 standard for 60 days [20]. For this purpose, the electrospun samples were cut into squares with dimensions of 1×1 cm^2, and their weight was measured on day zero. Then, the samples were placed in laboratory falcon tubes, and 5 mL of phosphate-buffered saline solution was added to each tube. The tubes were then incubated at a temperature of 37 ± 1 °C. After 24 h, the samples were removed from the tubes and immersed in distilled water to wash away the degradation particles. Subsequently, the samples were dried with filter paper and placed in a Petri dish (glass plate) and dried for 5 h in a vacuum oven at a temperature of 37.5 °C and a low pressure of about (14–16 Bar). The dry samples were weighed using a Sartorius 225D-1S balance (USA) with 1×10^{-5} accuracy. Five repetitions (n = 5) from all groups were evaluated at time intervals of 0, 1, 3, 5, 7, 14, 21, 30, 36, 42, 49, and 60 days. This evaluation was based on the percentage of weight loss over time, obtained using equation (1) [21]:

$$\%\text{Weight loss} = \frac{m_d - m_0}{m_0} \times 100 \tag{1}$$

Where m_d is the weight of the sample in the dry state on the day of the destruction calculation, and m_0 is the initial weight of the sample [21]. To evaluate the water absorption of electrospun scaffolds, samples were prepared in the form of small squares with dimensions of 10×10 mm^2 [22]. Initially, the dry samples were weighed (m_1) and placed individually in laboratory falcon tubes containing 5 ml of PBS solution for 24 h. Subsequently, the samples were removed and any adsorbed water on the sample surfaces was removed using filter paper at room temperature. Afterward, their weight was recorded (m_2). Then, using equation (2), the percentage of water absorption was calculated [22]:

$$\%\textit{Water absorption} = \frac{m_2 - m_1}{m_1} \times 100 \tag{2}$$

To measure the pH changes of the solutions containing PGS-PCL samples and to investigate the effect of RGO particles on the acidity and basicity of the solutions over a period of 60 days, a pH meter model AZ pH/mV/Temp.meter-86502 (Taiwan) was utilized. The surface resistance of the samples was assessed using the electrical conductivity test employing the four-point method. Initially, the samples were cut into thick strips (150–250 μm) and then brought into contact with four thin probes. Subsequently, a constant current ranging from 0.1 to 9 nA was passed through two external probes, and the electric potential was measured. The specific resistance (ρ) of the scaffold was calculated using equation (3), where L represents the distance between the two potential contacts, A denotes the cross-sectional area, and R signifies the electrical resistance [9,23]:

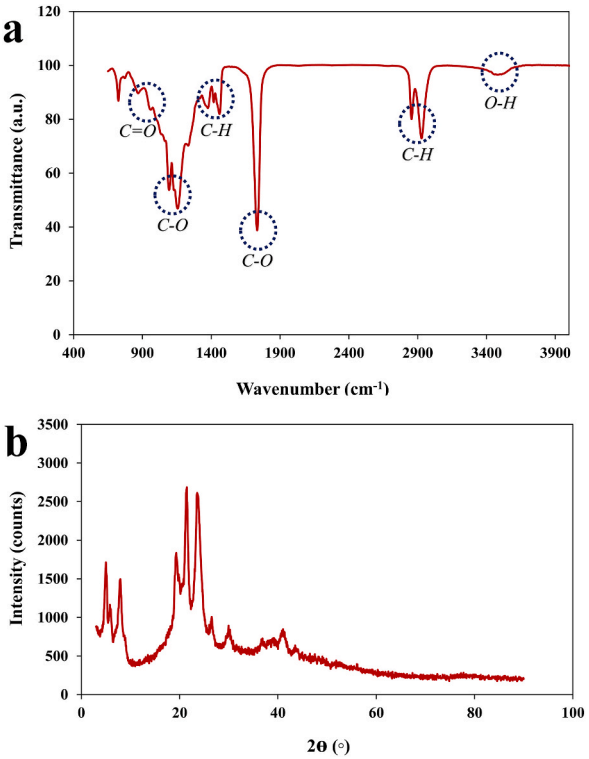

Fig. 2. a) FTIR spectrum and b) X-ray diffraction pattern of synthesized polyglycerol sebacate.

$$R = \rho\, L/A \tag{3}$$

Then σ (electrical conductivity (S/m)) was obtained with the help of equation (4) [9,23]:

$$\sigma = 1/\rho \tag{4}$$

The mechanical properties of the samples were assessed in accordance with ASTM-D882 standard using a Hounsfield-H25KS micro-tensile tester (England). The samples were prepared as strips with dimensions of 10 mm by 50 mm and an average thickness of 0.2 mm. Subsequently, the strip samples were clamped between the grips of the machine, and the tension test was conducted at a speed of 50 mm/min [9]. In this study, the MTT assay (according to ISO10993-5) was performed to determine the cell viability percentages and evaluate the metabolic activity of the HUVECs (third-passage cells were used for this study). An indirect method was employed; initially, three groups (S_1-S_3) with three repetitions (n = 3) were exposed to ultraviolet radiation (UV) for sterilization, and then an extract was prepared from each sample individually. Following the ISO10993-12 standard, an amount of sample sufficient to extract 0.1 g/mol in 1 ml of the culture medium was kept for 72 h in a humid atmosphere containing 95 % O_2/5 % CO_2 at a temperature of 37 °C in an incubator. Subsequently, the medium supernatant was removed and centrifuged. The primary extract (100 %) was diluted with culture medium (DMEM-F12 + 10 % FBS+1 % pen/strep) to concentrations of 50 % and 25 %. Then, 1 × 10^4 HUVECs were exposed to the prepared extracts at 37 °C in a humid atmosphere containing 95 % O_2/5 % CO_2 [24].

In this investigation, the cytotoxicity test (MTT) was conducted for three days, with three sample repetitions (n = 3) for each condition. After 1, 2, and 3 days of cell culture in a 24-well plate, the culture medium was aspirated, and the sample extract was incubated with MTT solution for 4 h to produce formazan crystals. Subsequently, the MTT solution was carefully aspirated, and to dissolve the formazan crystals, dimethylsulfoxide (DMSO) was added to the sample extracts and incubated at 37 °C for 1 h. Finally, 100 ml of the dissolved formazan solution was transferred to a 98-well plate, and the absorbance of the purple solution was measured using an ELISA reader Bio-Rad Model 680 instrument (Germany) at a wavelength of 490 nm. Cell viability was calculated using equation (5) [25]:

$$\text{Relative cell viability } (\%) = \frac{A_{sample} - A_b}{A_c - A_b} \times 100 \tag{5}$$

Where A_b is the absorption of the DMSO solution, A_{sample} is the absorption of the desired sample, and A_c is the adsorption of the control sample [25].

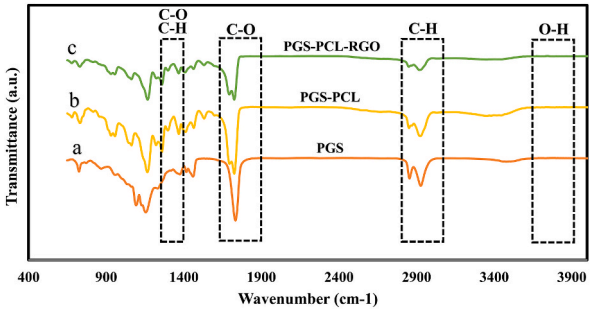

Fig. 3. FTIR spectra of composite scaffolds a) Synthesized PGS, b) PGS-PCL, c) PGS-PCL-RGO.

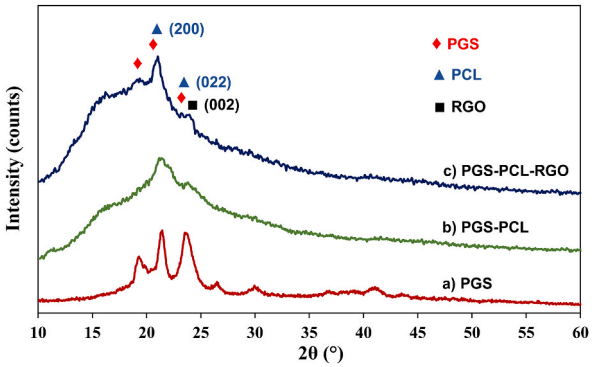

Fig. 4. X-ray diffraction pattern of composite scaffolds a) Synthesized PGS, b) PGS-PCL, c) PGS-PCL-RGO.

2.4. Statistical and image analysis

All statistical analyses were conducted on sample sizes ranging from at least 3 to a maximum of 5 cases. To assess the significance of the differences, values were determined ($*P < 0.05$). Statistical calculations were performed using SPSS version 22 software. Porosity percentage was measured using MATLAB version 8 (2013), and fiber diameters were measured using Image J version 44.1 software. The results were reported as mean ± standard deviation for each sample.

3. Results and discussion

3.1. Characterization of synthesized polyglycerol sebacate (PGS)

After synthesizing polyglycerol sebacate (PGS) to ensure the synthesis conditions, the polymer was characterized using FT-IR and XRD. According to the obtained FTIR spectrum (Fig. 2a), the peaks do not have any additional bonds indicating the remaining solvent or contamination in the composition, and the obtained spectrum is consistent with other references [26]. In the FTIR spectrum, peaks were observed at 1159 cm^{-1} and 1734 cm^{-1}, which are related to the presence of carbonyl and ester functional groups in the form of C-O and C=O, which indicates that this polymer is polyester. In addition, the resulting peak at 3449 cm^{-1} indicates that many hydroxyl groups (O-H), directly attached to the main chain have hydrogen bonds and lead to the hydrophilic properties of this polymer. The peak at 931 cm^{-1} is related to sebacic acid. Also, the peaks related to the alkyl group at 2857 cm^{-1}, 2927 cm^{-1}, and 1376 cm^{-1} represent the resonances of the CH and CH_2 groups [26]. According to Fig. 2b, the XRD pattern was related to polyglycerol sebacate and this pattern showed that the structure of this polymer was semi-crystalline. According to the study of Fakhrali et al. [27] for pure PGS, two main peaks were reported at 19.3 and 23°, which were observed in the resulting pattern. In the research of Ghafaralahi et al. [9] the XRD analysis of PGS elastomer confirmed the correctness of the synthesis and the X-ray diffraction pattern of PGS showed that the semi-crystalline phase is almost dominant. Therefore, based on the results of the XRD analyses related to this material, it is concluded that the synthesized PGS is consistent with other references.

3.2. Evaluation of PGS-PCL-RGO composite scaffolds

Fig. 3 shows the FTIR spectra for synthesized PGS, PGS-PCL, and PGS-PCL-RGO. The FTIR spectrum of the synthesized PGS is shown in Fig. 3a. This spectrum is also shown in Fig. 2, and detailed explanations regarding this spectrum are provided in the description for Fig. 2. It is included here for comparison with other spectra. According to Fig. 3b, which illustrates the spectroscopy of the PGS-PCL

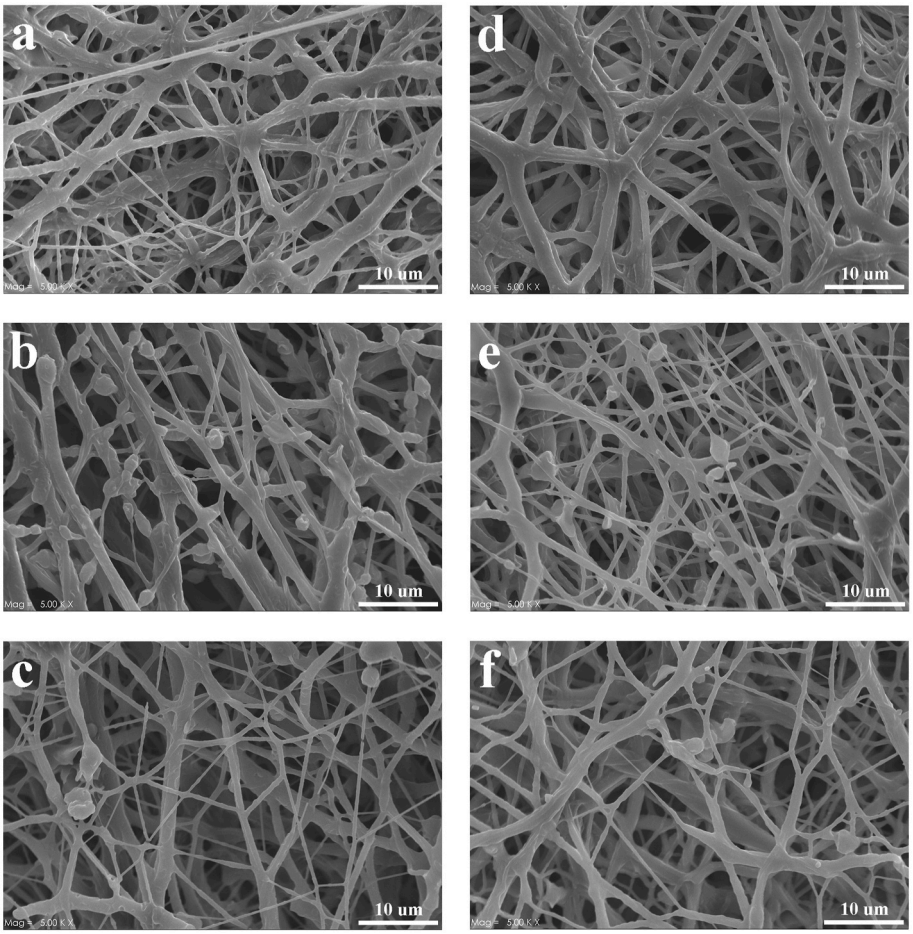

Fig. 5. SEM images of composite scaffolds. a: 33%PGS-67%PCL, b: 33%PGS-66%PCL-1%RGO, c: 33%PGS-65%PCL-2%RGO d: 50%PGS-50%PCL, e: 49%PGS-50%PCL-1%RGO, f: 48%PGS-50%PCL-2%RGO.

Table 2
Average diameter and porosity of composite scaffolds.

Sample	Average diameter (μm)	Porosity (%)
%33PGS-%67 PCL	2.236 ± 0.577	87.4
%33 PGS-%66 PCL-%1RGO	0.957 ± 0.234	85.75
%33 PGS-%65PCL-%2RGO	0.590 ± 0.150	85.77
%50PGS-%50 PCL	1.202 ± 0.378	86.78
%49PGS-%50PCL-%1RGO	0.690 ± 0.162	84.37
%48PGS-%50PCL-%2RGO	0.441 ± 0.158	82.97

composite scaffold, evidence related to the presence of polycaprolactone in the composition was obtained. Alkyl group peaks can be observed at 1297 cm^{-1}, 2853 cm^{-1}, and 2929 cm^{-1}, while ester peaks were visible at 1724 cm^{-1} and 1250 cm^{-1}. The obtained results are consistent with other studies conducted on PGS-PCL infrared spectroscopy. The corresponding peak at 3444 cm^{-1} indicates the O-H group in the composition of PGS, suggesting the high hydrophilicity of this polymer [17]. By adding RGO to the composite composition according to Fig. 3c, which depicts PGS-PCL-RGO, the peak of stretching vibrations of O-H groups at 3400 cm^{-1} was absent due to deoxygenation, indicating the presence of RGO in the composition. Additionally, a stretching vibration was observed at around 2800 cm^{-1}, which indicates the presence of C-H groups in RGO. The presence of RGO in the PGS-PCL-RGO composite scaffold is confirmed according to the results obtained from the FTIR spectrum, and it aligns with findings from other sources [28].

Fig. 4 shows the XRD patterns for PGS, PGS-PCL, and PGS-PCL-RGO. As indicated in Fig. 4a, PGS exhibits a semi-crystalline structure. Although PGS is typically amorphous, synthesis conditions such as time, temperature, and pressure can affect its structure, potentially leading to a semi-crystalline form. For the PGS-PCL composite, the XRD pattern remains semi-crystalline; since PCL is also a semi-crystalline polymer, its presence alongside PGS maintains the semi-crystalline structure. Two main PCL peaks are observed

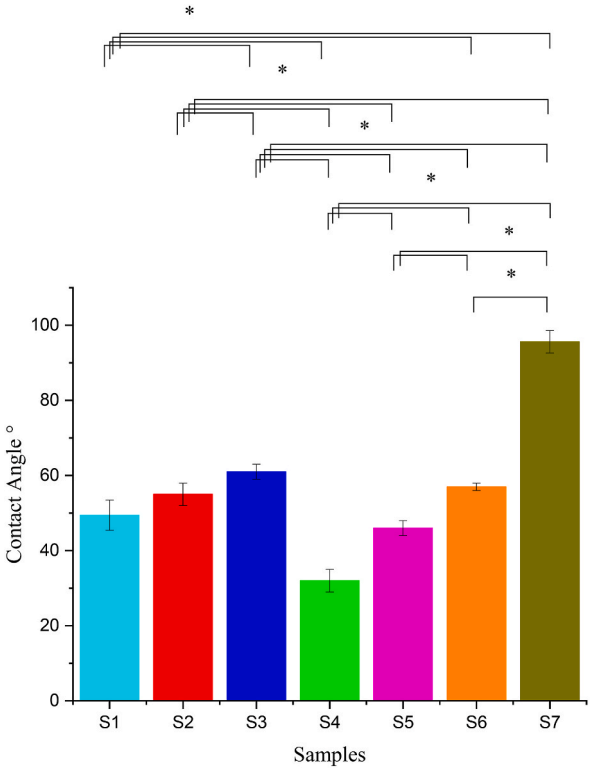

Fig. 6. Water contact angles for composite scaffolds with different compositions (*$P < 0.05$). S_1:33%PGS-67%PCL, S_2:33%PGS-66%PCL-1%RGO, S_3:33%PGS-65%PCL-2%RGO S_4:50%PGS-50%PCL, S_5:49%PGS-50%PCL-1%RGO, S_6:48%PGS-50%PCL-2%RGO, S_7:PCL.

Table 3
Results of measuring the electrical conductivity of scaffolds.

Chemical composition of scaffold	Cross section of Scaffold (mm)	Scaffold thickness (mm)	Potential double contact distance, L (mm)	The average resistance of the scaffold, R (Ω)	Electrical conductivity, σ (S/m)
%33PGS-%67 PCL	10	0.168	6.7	114675	58E-4
%33 PGS-%66 PCL-%1RGO	6.9	0.140	6.3	25157	36E-3
%33 PGS-%65PCL-%2RGO	8.75	0.058	5.1	11254	51E-3
%50PGS-%50 PCL	5.25	0.117	5.5	74345	14E-3
%49PGS-%50PCL-%1RGO	8.96	0.064	5.3	15080	39E-3
%48PGS-%50PCL-%2RGO	8.5	0.145	5.5	14791	43E-3

at $2\theta = 21.3^\circ$ and $2\theta = 23.7^\circ$, with Miller index (200) and (022) respectively, consistent with other references [27]. In Fig. 4c, in addition to these peaks, a peak around $2\theta = 25.5^\circ$ is visible, corresponding to RGO with a Miller index of (002). Due to reduced oxidation, this peak may be weaker and broader compared to graphene oxide (GO).

Fig. 5a to f displays SEM images of composite scaffolds with reduced graphene oxide (RGO) and scaffolds without reduced graphene oxide. The images suggest that the presence of RGO has reduced the diameter of the fibers (the values are listed in Table 2), potentially due to the electrical conductivity of this material. When RGO is subjected to an electrostatic field, it results in the alignment of fibers in the same direction and consequently decreases the fiber diameter [29]. Examination of PGS-PCL-RGO scaffolds reveals that the reduced graphene oxide ceramic particles are uniformly dispersed in the polymer matrix, with minimal agglomeration of RGO particles. In Table 2, along with the average fiber diameters for the samples, the porosity of the composite scaffolds is reported. The results indicate that the viscosity of the polymer solution increased with the rise in the RGO ratio, leading to a decrease in fiber diameter. Consequently, fibers with smaller diameters and greater uniformity were produced [30].

According to the studies by Kharaziha et al. [17], hydrophilicity is suitable for cell adhesion, proliferation, and penetration in the desired materials, especially in tissue engineering applications. Based on the obtained results (Fig. 6), the pure PCL sample (S_7) had the highest contact angle ($95.6 \pm 3^\circ$) due to its hydrophobic nature, which aligns with findings in some research articles [9,27,31]. The

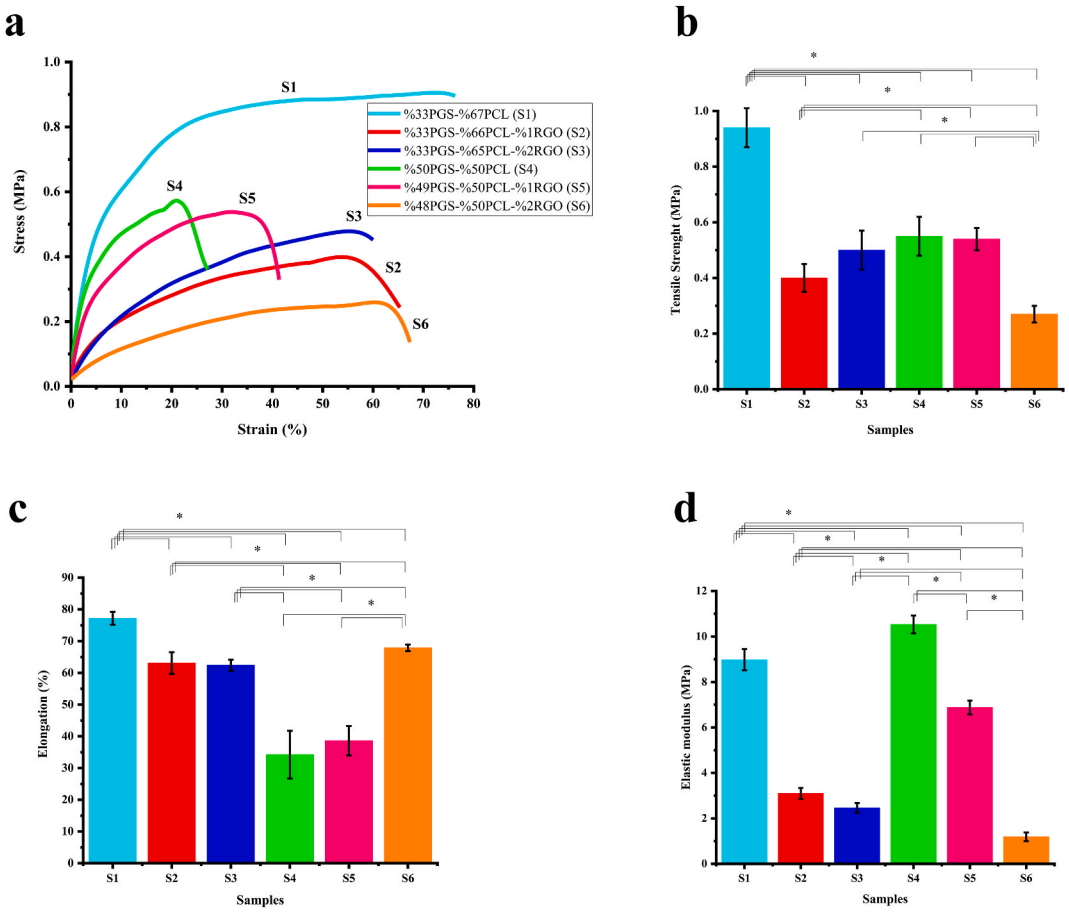

Fig. 7. a) stress-strain curve, b) tensile strength values, c) Elongation values, and d) elastic modulus values of composite scaffolds. S_1:33%PGS-67% PCL, S_2:33%PGS-66%PCL-1%RGO, S_3:33%PGS-65%PCL-2%RGO S_4:50%PGS-50%PCL, S_5:49%PGS-50%PCL-1%RGO, S_6:48%PGS-50%PCL-2%RGO.

contact angle of this polymer can be improved by adding hydrophilic polymers to it. The results indicate that by adding 33 % (S_1) and 50 % (S_4) of polyglycerol sebacate (PGS) to polycaprolactone (PCL), the water contact angle decreased to 49±4° and 32±3°, respectively, due to the hydrophilic nature of PGS caused by the presence of hydroxyl groups attached to carbon. The high level of hydrophilicity of the scaffolds can also be related to the morphology of the fibers; when the fibers are non-uniform, the contact surface ratio increases, leading to greater absorption and hydrophilicity [17]. Additionally, increased surface roughness can enhance hydrophilicity [32]. Therefore, several factors, such as morphology, fiber diameter, and physicochemical properties, influence hydrophilicity. By adding 1 % reduced graphene oxide (RGO) to the 33%PGS-66%PCL-1%RGO (S_2) and 49%PGS-50%PCL-1%RGO (S_5) samples, the contact angle increased to 55±3° and 46±2°, respectively. Moreover, due to the hydrophobic nature of RGO compared to GO, adding 2%wt RGO to the 33%PGS-65%PCL-2%RGO (S_3) and 48%PGS-50%PCL-2%RGO (S_6) scaffolds increased the contact angle to 61±2° and 57±1°, respectively. According to the research by Ghafaralahi et al. [9], tissue engineering substrates generally need a proper balance of hydrophilicity and hydrophobicity. Excessively hydrophobic surfaces increase cellular affinity but decrease biocompatibility, whereas surfaces with high hydrophilicity exhibit fewer cellular interactions. Thus, contact angles of 45–70 or 30–60° can be suitable for tissue engineering. Considering these factors, the 33%PGS-65%PCL-2%RGO (S_3) sample appears to have the optimal contact angle for tissue engineering.

The electrical conductivity of the scaffold is crucial in heart tissue engineering. Table 3 presents the conductivity of the measured samples. Based on the obtained results, the electrical conductivity of scaffolds is 33%PGS-67%PCL (58E-4 S/m) and 50 % PGS-50%PCL (14E-3 S/m). By adding 1%wt of RGO to the composite scaffolds, the electrical conductivity of the scaffolds in S_2 and S_5 increased by approximately 520 % and 178 %, respectively. Similarly, by adding 2%wt of RGO in S_3 and S_6, the conductivity increased by about 780 % and 207 %, respectively. The presence of RGO and increasing its amount in the scaffolds has led to an increase in electrical conductivity, attributed to the presence and formation of negative functional groups on the RGO plates [9]. In this study, reduced graphene oxide particles were added to the polymer matrix as reinforcement to impart electrical conductivity to the scaffold. In the utilization of conductors, various factors, including the concentration of the conductor, directly influence the control of the electrical conductivity of the composite. Therefore, in composite materials, a critical concentration of reinforcement is important, where interactions between the reinforcing phase and the background phase are in equilibrium, facilitating the electron transfer process to the

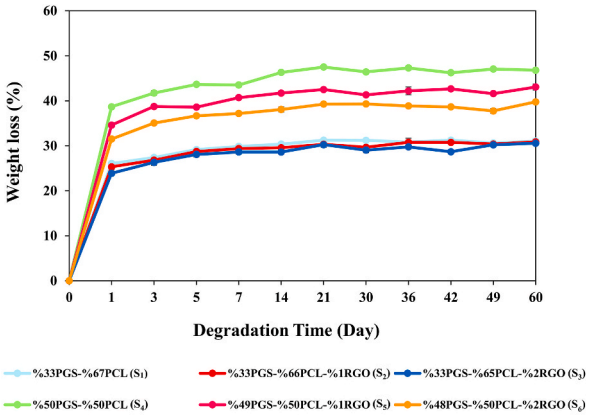

$p < 0.05$					
S_1:S_4	S_2:S_4	S_3:S_4	S_4:S_1	S_5:S_1	S_6:S_1
S_1:S_5	S_2:S_5	S_3:S_5	S_4:S_2	S_5:S_2	S_6:S_2
S_1:S_6	S_2:S_6	S_3:S_6	S_4:S_3	S_5:S_3	S_6:S_3
-	-	-	S_4:S_5	S_5:S_4	S_6:S_4
-	-	-	S_4:S_6	S_5:S_6	S_6:S_5

Fig. 8. Weight loss of composite scaffolds over 60 days. S_1:33%PGS-67%PCL, S_2:33%PGS-66%PCL-1%RGO, S_3:33%PGS-65%PCL-2%RGO S_4:50% PGS-50%PCL, S_5:49%PGS-50%PCL-1%RGO, S_6:48%PGS-50%PCL-2%RGO.

matrix. The results of Baheiraei et al.'s studies [33,34] indicated that the electrical conductivity of heart muscle tissue ranges from 16 $\times 10^{-2}$ to 50 $\times 10^{-2}$ S/m. However, other research suggests that for tissue engineering applications, conductivity values within the semiconductor range between 10^{-6} and 10^{2} S/m are sufficient [35]. The family of graphene materials, including RGO, is more effective in improving electrical conductivity compared to other reinforcing nanoparticles such as carbon nanotubes (CNT/CNF) [36]. Based on the results of Park et al.'s studies [15,16], incorporating graphene nanosheets with electrical conductivity properties into cells enhances cell-cell and cell-ECM (extracellular matrix) communication. Therefore, considering the results, the value of 2%wt was deemed the optimal concentration, and the composite scaffold of 33%PGS-65%PCL-2%RGO (S_3) exhibits the highest electrical conductivity (51E-3 S/m).

According to Fig. 7, the mechanical properties of composite scaffolds fabricated via the electrospinning method and the impact of 1:1 and 1:2 PGS-PCL weight ratios, as well as the amounts of 1%wt and 2%wt RGO, on the mechanical performance of the scaffolds were investigated using a tensile test. Providing suitable mechanical properties is one of the fundamental requirements for scaffolds used in myocardial tissue engineering, as they play a crucial role in cell adhesion and cell growth. According to studies by Fakhrali et al. [27], the elastic modulus (E), ultimate tensile strength (UTS), and elongation (EL) are correlated with hardness, strength, and elasticity, respectively. After plotting stress-strain curves (Fig. 7a), values of tensile strength (Fig. 7b), elongation (Fig. 7c), and elastic modulus (Fig. 7d) of composite scaffolds were obtained. According to Fig. 6b, the 33%PGS-67%PCL scaffold (S_1) exhibited the highest tensile strength (approximately 0.94 MPa). Generally, scaffolds without any reinforcing particles (S_1 and S_4) demonstrated more strength due to the larger diameter and better uniformity of the fibers.

Additionally, an increase in the strain rate leads to material hardening and, consequently, an increase in scaffold strength. Conversely, reducing the amount of PCL (S_4) resulted in decreased strength, consistent with findings from other studies [27]. The addition of RGO to the polymer matrix decreased tensile strength (S_2 and S_3). One reason for the reduced strength in reinforced scaffolds with RGO is the smaller fiber diameter; when polymer composite scaffolds are reinforced by RGO particles, the fiber diameter decreases, leading to lower strength. Nano-reduced graphene oxide reinforcement can enhance tensile behavior due to its high surface-to-volume ratio and suitable mechanical properties. However, the reinforcement amount should be optimized to maintain mechanical properties; adding non-optimal reinforcement particles to the polymeric matrix can result in RGO particle agglomeration and create stress concentration points. Therefore, the tensile strength in the 33%PGS-66%PCL-1%RGO scaffold (S_2) is approximately 0.4 MPa, and in the 33%PGS-65%PCL-2%RGO scaffold (S_3) is about 0.5 MPa, representing a decrease in strength by 88 % and 57.44 %, respectively, compared to similar samples without particles (S_1). However, the improved mechanical properties of S_3 compared to S_2 (approximately a 25 % increase) suggest that despite increased particle percentage and aggregation, the high surface-to-volume ratio of particles contributed to higher strength. According to previous studies, adding more than 2%wt RGO may lead to increased particle agglomeration and weakened mechanical properties, making it unsuitable for tissue engineering [9]. In the 50%PGS-50%PCL scaffold (S_4), compared to the 33%PGS-67 PCL scaffold (S_1), the tensile strength decreased by about 43 % due to the elastomeric property of PGS. Therefore, as the weight percentage of polyglycerol sebacate increases, the tensile strength decreases. On the other hand, the strength of the 49%PGS-50PCL-1%RGO scaffold (S_5) increased by about 100 % compared to the 48%PGS-50%PCL-2%RGO scaffold (S_6). With an increase in the percentage of polyglycerol sebacate in the composite, the particle distribution minimized, and by increasing RGO up to approximately 2%wt, the agglomeration of RGO particles and stress concentration centers likely increased, resulting in decreased tensile strength. Fig. 6c shows that S_1 had the highest elongation (77.2 %), and S_4 the lowest (34.24 %).

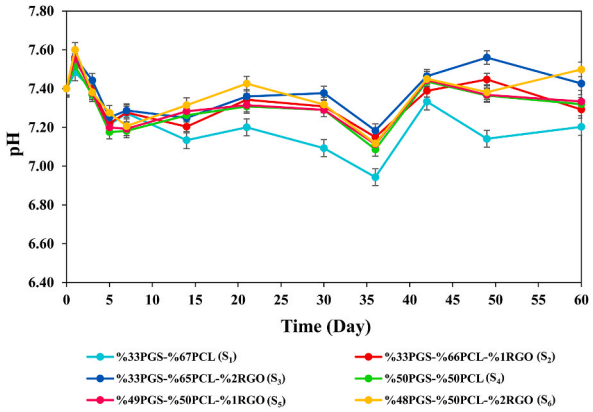

Fig. 9. The pH changes in composite scaffolds over 60 days. S_1:33%PGS-67%PCL, S_2:33%PGS-66%PCL-1%RGO, S_3:33%PGS-65%PCL-2%RGO S_4:50%PGS-50%PCL, S_5:49%PGS-50%PCL-1%RGO, S_6:48%PGS-50%PCL-2%RGO.

According to the article by Jia et al. [7], the maximum elongation for human heart tissue ranges from 20 % to 90 %, with an average of 60 %. Additionally, studies indicate that a minimum elongation of 20 % is required for cardiomyocyte growth. S_1 with a 1:1 PGS-PCL weight ratio exhibited more elongation than S_4 with a 1:2 PGS-PCL weight ratio. The increase in polyglycerol sebacate, owing to its elastomeric property, led to increased elongation. However, in S_4 (50%PGS-50%PCL) compared to S_1 (33%PGS-67%PCL), elongation decreased with the addition of PGS due to the decreased PCL amount from 67 % to 50 %. Notably, there was no significant difference between S_2 and S_3, and the addition of 1 % RGO increased the elongation of S_5 compared to S_4. Moreover, the elongation of S_6 significantly increased with the addition of 2 wt% RGO, compared to S_2 and S_3 (approximately 65 %). Although the elongation decreased with the addition of RGO, this value falls within the range suitable for heart tissue. The primary goal of tissue engineering is to replicate the structure and properties of the desired tissue. Therefore, samples without reduced graphene oxide (S_1) and those with reduced graphene oxide (S_2, S_3, and S_6) can mimic the elongation of heart tissue. As reported in previous articles [37], the modulus of the human cardiac muscle at the end of cardiac expansion ranges from 0.2 to 0.5 MPa. According to Fig. 6d, S_6 exhibits the lowest modulus (1.19 MPa), indicating the least brittleness. In samples S_1 and S_4, the modulus of elasticity was 8.98 and 10.53 MPa, respectively. These values significantly differ from the modulus of elasticity of myocardial tissue. With the addition of RGO to these scaffolds, the modulus of elasticity decreased; the values for S_2, S_3, and S_6 were 1.19, 2.46, and 3.1 MPa, respectively. These values closely mimic the required elasticity modulus of heart muscle. In general, the 33%PGS-65%PCL-2%RGO composite scaffold (S_3) with suitable mechanical properties can be an ideal choice as a cardiac tissue engineering scaffold.

According to Fig. 8, generally, the samples exhibit a high degradation rate until the first day. Subsequently, the degradation rate increases steadily until the 60th day with a very low slope. The rapid degradation on the first day is likely a result of high water absorption, leading to the disintegration of the amorphous parts of the structure. Semi-crystalline structures, such as polycaprolactone, degrade later than amorphous structures like polyglycerol sebacate.

As per in vitro studies by Sundback and Wang [38,39], PGS undergoes severe surface degradation, with the bulk of the material remaining unaffected by erosion, which aligns with the rapid degradation process observed on the first day. The weight loss after 60 days for S_1 was 26.06 %. By adding 1%wt and 2%wt of RGO to the samples (S_2 and S_3), the weight loss percentages of S_2 and S_3 reached 25.32 % and 23.87 %, respectively. The reduction in the degradation process can be attributed to the hydrophobic nature of RGO, which slows down the degradation rate. As depicted in Fig. 8, increasing PGS to 50 % in S_4 resulted in higher degradation rate and weight loss compared to samples with a lower percentage of PGS (S_5 and S_6) ($P < 0.05$). This is due to the hydrophilic nature and semi-crystalline structure of PGS [40]. Meanwhile, S_5 and S_6 incorporate hydrophobic RGO particles [41], which reduced weight loss percentages to 34.59 % and 31.50 %, respectively, compared to S_4. One significant aspect of the degradation test is cell viability. Since endothelial cells require around 1 week to 10 days for growth, the scaffold should not degrade quickly during this period to ensure proper anchoring, growth, and cell proliferation. Therefore, it appears that among the samples without reduced graphene oxide, the 33%PGS-67%PCL composite scaffold (S_1), and among the samples with reduced graphene oxide, the 33%PGS-65%PCL-2%RGO composite scaffold (S_3) are more suitable options than the others.

Fig. 9 illustrates the trend of pH changes in composite scaffolds over a 60-day degradation period. Generally, pH changes vary across different days for all samples, with the range of changes being lower for the sample containing RGO particles. However, this variation increases for composite samples with higher PGS values. Notably, the pH change range for samples S_2 and S_3 falls within the pH range of heart tissue. In a study by Schroeder et al. [42], intracellular pH in the heart was measured using CO_2 and hyperpolarized bicarbonate, revealing a normal pH of around 7.1–7.2 for heart muscle. Heart complications, such as ischemia, often lead to rapid onset acidosis during myocardial diseases. Reduced coronary artery perfusion triggers anaerobic glycolysis, resulting in increased intracellular protons and lactic acid accumulation in both intracellular and extracellular spaces. These react with HCO_3 to form CO_2, further contributing to the already produced CO_2 from oxidative metabolism. This accumulation of protons, lactic acid, and CO_2 causes a decrease in intracellular pH (pHi) from the normal levels of 7.1–7.2.

A study by Chen et al. [43] demonstrated that degradation products of PGS in PBS solution exhibit no toxic effects and are naturally

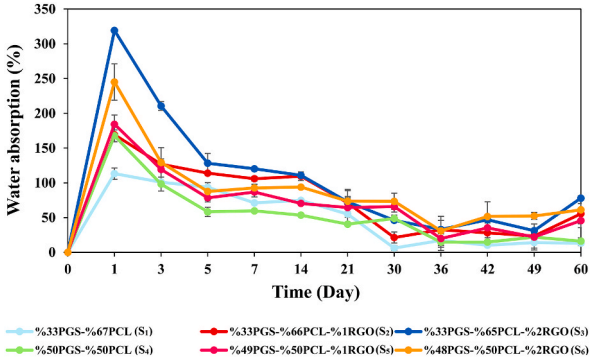

Fig. 10. Water absorption of composite scaffolds over 60 days. S_1:33%PGS-67%PCL, S_2:33%PGS-66%PCL-1%RGO, S_3:33%PGS-65%PCL-2%RGO S_4:50%PGS-50%PCL, S_5:49%PGS-50%PCL-1%RGO, S_6:48%PGS-50%PCL-2%RGO.

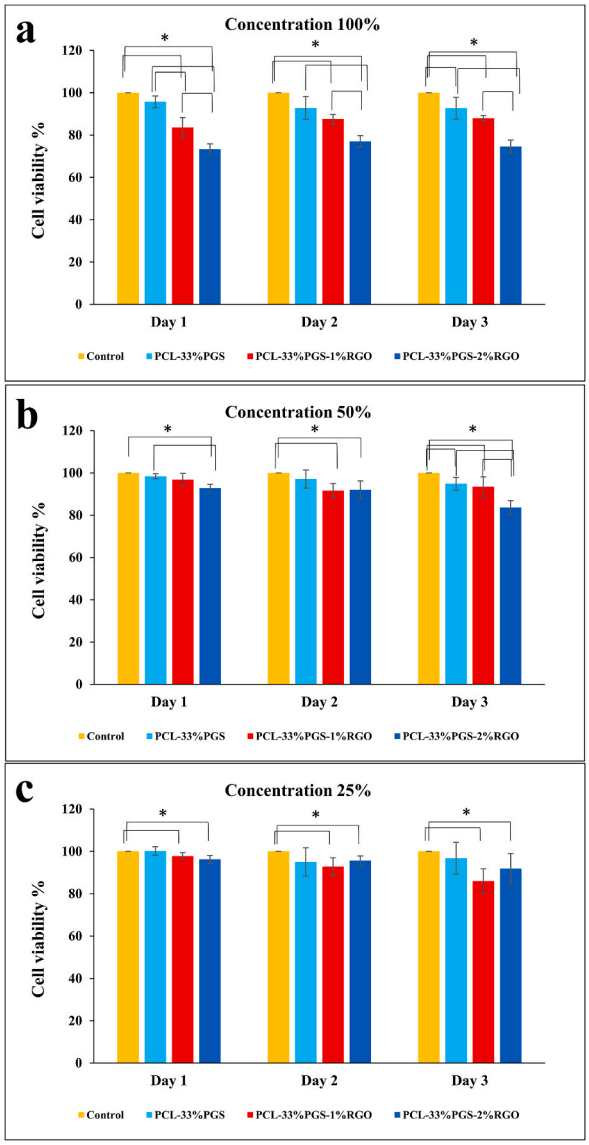

Fig. 11. The MTT assay results after 1, 2, and 3 days at (a) 100 %, (b) 50 %, and (c) 25 % concentrations for S_1 to S_3 (*$P < 0.05$). S_1:33%PGS-67% PCL, S_2:33%PGS-66%PCL-1%RGO, S_3:33%PGS-65%PCL-2%RGO.

metabolized in the body. Additionally, Ghafaralahi et al. [9] highlighted that the degradation of polycaprolactone in physiological conditions, such as within the human body, does not pose any toxic effects, making it highly suitable for use as an implantable biological material.

Simultaneously with the degradation test, the water absorption rate of the scaffolds was also measured. This process was investigated over a period of up to 60 days. According to Fig. 10, on the first day, the sample with a 1/2 PGS-PCL ratio (S_1) had approximately 113 % water absorption. When the PGS-PCL ratio becomes 1:1 and the amount of PGS reaches 50 % (S_4), the hydrophilicity increases due to the presence of PGS hydrophilic groups. Consequently, the penetration of water into the scaffold becomes easier because of the presence of hydroxyl groups [27], and the amount of water absorption in S_4 reached 167.86 %. The results show that with the addition of 2 % RGO compared to 1 %, the amount of water absorption increases. This is probably due to the residues of oxygen-containing functional groups during the process of reducing RGO by GO [44]. From the fifth day onwards, the water absorption process decreased significantly and remained within a certain range until the end of the 60 days.

Based on the data evaluations so far, S_1, S_2, and S_3 composite scaffolds have been selected for cytotoxicity evaluation (MTT assay). Fig. 11a shows the comparison of HUVEC viability percentages between the control sample and extracts of S_1, S_2, and S_3 at 100 % concentration. On the first day, S_1 and S_2 exhibited the highest cell viability, with a significant difference compared to the control ($P < 0.05$). S_3, containing the most RGO (2 % wt), had lower cell viability but still demonstrated good biocompatibility, with its difference from the other samples being significant ($P < 0.05$). A similar trend was observed on the second and third days, indicating that the composite samples have good cellular compatibility. At 50 % extract concentration, all three samples showed significant cell growth and did not cause any toxicity. On the first day, S_3 had a significant difference in cell viability compared to S_1 ($P < 0.05$), but no significant difference compared to S_2. Additionally, there was no significant difference between S_1 and S_2. On the third day, significant cell growth was observed, with the samples showing a significant difference ($P < 0.05$). This indicates that cell growth in the samples is acceptable, with the third day being similar to the first day. When the extract concentration was reduced to 25 %, all samples maintained good cell viability on the first, second, and third days. Notably, S_3 exhibited a higher cell growth rate than S_2 on the second and third days. These results suggest that, according to the cytotoxicity evaluation, the most suitable scaffold is a composite containing 1 %–2 % RGO. In fact, at lower extract concentrations (as shown in Fig. 11b and c), cell growth and proliferation improved. Specifically, cell proliferation for the 33 % PGS - 65 % PCL - 2 % RGO composite scaffold (S_3) increased significantly, likely due to the lower amount of degradation products.

4. Conclusion

In this research, polyglycerol sebacate (PGS) was synthesized using the poly-condensation technique, and composite scaffolds consisting of polyglycerol sebacate, polycaprolactone (PCL), and reduced graphene oxide (RGO) particles were fabricated using the electrospinning method. Morphological, mechanical, physicochemical, electrical, and biocompatibility evaluations of the scaffolds were then performed. In the chemical characterization of PGS based on the FTIR test, it was found that this polymer was correctly synthesized and had ester, hydroxyl, and carbonyl-carboxyl bonds without any additional bonds due to the presence of solvents or additional compounds. The optimal combination of PGS-PCL to make a composite scaffold suitable for heart tissue was a 1:2 wt ratio (33%wt PGS-67%wt PCL), and the most suitable solvents for creating favorable properties, including the suitable morphology of fibers, were chloroform and acetone. The optimal parameters for the electrospinning process were a rate of 1 ml/h, a voltage of 18 kV, and a distance of 17 cm. Findings from SEM indicated that the presence of RGO reduced the diameter of the fibers. In the contact angle test, the 33 % PGS-66 % PCL-2% RGO composite scaffold had a value of $61 \pm 2^{\circ}$, indicating the high hydrophilicity of the scaffold and its important role in cell adhesion, which is due to the presence of RGO. The tensile test showed that the 33 % PGS-65 % PCL-2% RGO composite scaffolds had a tensile strength of 0.5 MPa, an elongation of 62.43 %, and an elastic modulus of 2.46 MPa. These mechanical test values are suitable for myocardial tissue engineering. The electrical conductivity test showed that by adding 2%wt of RGO to the 33 % PGS-65 % PCL-2% RGO composite scaffold, the highest electrical conductivity (51E-3 S/m) was obtained. This conductivity is suitable for heart tissue engineering. Cytotoxicity evaluation (MTT assay) showed that the 33%PGS-65%PCL-2%RGO composite scaffold in different extract concentrations promoted favorable cell viability. According to the obtained results, it is concluded that the composite scaffold with the combination of 33 % PGS-65 % PCL-2% RGO can be an ideal candidate for use in myocardial tissue engineering.

Data availability statement

Supporting data for this study may be available and will be considered upon reasonable request.

CRediT authorship contribution statement

Azadeh Rejali: Writing – original draft, Methodology, Investigation, Formal analysis. **Mehdi Ebrahimian-Hosseinabadi:** Writing – review & editing, Supervision, Resources, Project administration, Methodology, Conceptualization. **Anousheh Zargar Kharazi:** Writing – review & editing, Supervision, Project administration, Methodology, Investigation, Conceptualization.

Declaration of competing interest

The authors declare that they have no known competing financial interests or personal relationships that could have appeared to

influence the work reported in this paper.

Acknowledgments

The authors acknowledge the support of the University of Isfahan (UI) and Isfahan University of Medical Sciences (IUMS) in IRAN.

Appendix A. Supplementary data

Supplementary data to this article can be found online at https://doi.org/10.1016/j.heliyon.2024.e38672.

References

[1] D. Mozaffarian, E.J. Benjamin, A.S. Go, D.K. Arnett, M.J. Blaha, M. Cushman, M.B. Turner, Heart disease and stroke statistics—2016 update: a report from the American Heart Association, Circulation 133 (4) (2016) e38–e360, https://doi.org/10.1161/CIR.0000000000000350.
[2] V. Sharma, S.K. Dash, K. Govarthanan, R. Gahtori, N. Negi, M. Barani, S. Ojha, Recent advances in cardiac tissue engineering for the management of myocardium infarction, Cells 10 (10) (2021) 2538, https://doi.org/10.3390/cells10102538.
[3] P. Gil-Cabrerizo, I. Scacchetti, E. Garbayo, M.J. Blanco-Prieto, Cardiac tissue engineering for myocardial infarction treatment, Eur. J. Pharmaceut. Sci. 185 (2023) 106439, https://doi.org/10.1016/j.ejps.2023.106439.
[4] M.W. Rasheed, A. Mahboob, I. Hanif, An estimation of physicochemical properties of heart attack treatment medicines by using molecular descriptor's, South Afr. J. Chem. Eng. 45 (2023) 20–29, https://doi.org/10.1016/j.sajce.2023.04.003.
[5] R. Coronel, R. Wilders, A.O. Verkerk, R.F. Wiegerinck, D. Benoist, O. Bernus, Electrophysiological changes in heart failure and their implications for arrhythmogenesis, Biochim. Biophys. Acta, Mol. Basis Dis. 1832 (12) (2013) 2432–2441, https://doi.org/10.1016/j.bbadis.2013.04.002.
[6] A. Ghofrani, L. Taghavi, B. Khalilivavdareh, A.R. Shirvan, A. Nouri, Additive manufacturing and advanced functionalities of cardiac patches: a review, Eur. Polym. J. 174 (2022) 111332, https://doi.org/10.1016/j.eurpolymj.2022.111332.
[7] Y. Jia, W. Wang, X. Zhou, W. Nie, L. Chen, C. He, Synthesis and characterization of poly (glycerol sebacate)-based elastomeric copolyesters for tissue engineering applications, Polym. Chem. 7 (14) (2016) 2553–2564, https://doi.org/10.1039/C5PY01993A.
[8] R. Rai, M. Tallawi, A. Grigore, A.R. Boccaccini, Synthesis, properties and biomedical applications of poly (glycerol sebacate)(PGS): a review, Prog. Polym. Sci. 37 (8) (2012) 1051–1078, https://doi.org/10.1016/j.progpolymsci.2012.02.001.
[9] S. Ghafaralahi, M. Ebrahimian-Hosseinabadi, A. Zargar Kharazi, Poly (glycerol-sebacate)/poly (caprolactone)/graphene nanocomposites for nerve tissue engineering, J. Bioact. Compat Polym. 33 (5) (2018) 529–542, https://doi.org/10.1177/0883911518793912.
[10] R. Rai, M. Tallawi, C. Frati, A. Falco, A. Gervasi, F. Quaini, A.R. Boccaccini, Bioactive electrospun fibers of poly (glycerol sebacate) and poly (ε-caprolactone) for cardiac patch application, Adv. Healthcare Mater. 4 (13) (2015) 2012–2025, https://doi.org/10.1002/adhm.201500154.
[11] G.V. Novakovic, T. Eschenhagen, C. Mummery, Myocardial tissue engineering: in vitro models, Cold Spring Harbor perspectives in medicine 4 (3) (2014).
[12] L.M. Monteiro, F. Vasques-Nóvoa, L. Ferreira, P. Pinto-do-Ó, D.S. Nascimento, Restoring heart function and electrical integrity: closing the circuit, NPJ Regenerative medicine 2 (1) (2017) 9, https://doi.org/10.1038/s41536-017-0015-2.
[13] A. Bagri, C. Mattevi, M. Acik, Y.J. Chabal, M. Chhowalla, V.B. Shenoy, Structural evolution during the reduction of chemically derived graphene oxide, Nat. Chem. 2 (7) (2010) 581–587, https://doi.org/10.1038/NCHEM.686.
[14] A.T. Smith, A.M. LaChance, S. Zeng, B. Liu, L. Sun, Synthesis, properties, and applications of graphene oxide/reduced graphene oxide and their nanocomposites, Nano Materials Science 1 (1) (2019) 31–47, https://doi.org/10.1016/j.nanoms.2019.02.004.
[15] J. Park, Y.S. Kim, S. Ryu, W.S. Kang, S. Park, J. Han, B.S. Kim, Graphene potentiates the myocardial repair efficacy of mesenchymal stem cells by stimulating the expression of angiogenic growth factors and gap junction protein, Adv. Funct. Mater. 25 (17) (2015) 2590–2600, https://doi.org/10.1002/adfm.201500365.
[16] M.H. Norahan, M. Pourmokhtari, M.R. Saeb, B. Bakhshi, M.S. Zomorrod, N. Baheiraei, Electroactive cardiac patch containing reduced graphene oxide with potential antibacterial properties, Mater. Sci. Eng. C 104 (2019) 109921, https://doi.org/10.1016/j.msec.2019.109921.
[17] A.Z. Kharazi, M. Atari, E. Vatankhah, S.H. Javanmard, A nanofibrous bilayered scaffold for tissue engineering of small-diameter blood vessels, Polym. Adv. Technol. 29 (12) (2018) 3151–3158, https://doi.org/10.1002/pat.4437.
[18] Z. Wu, Q. Li, L. Wang, Y. Zhang, W. Liu, S. Zhao, Y. Fan, A novel biomimetic nanofibrous cardiac tissue engineering scaffold with adjustable mechanical and electrical properties based on poly (glycerol sebacate) and polyaniline, Materials Today Bio 23 (2023) 100798, https://doi.org/10.1016/j.mtbio.2023.100798.
[19] C. Xu, K. Yang, Y. Xu, X. Meng, Y. Zhou, Y. Xu, N. Dong, Melt-electrowriting-enabled anisotropic scaffolds loaded with valve interstitial cells for heart valve tissue Engineering, J. Nanobiotechnol. 22 (1) (2024) 378, https://doi.org/10.1186/s12951-024-02656-5.
[20] S.L. Liang, X.Y. Yang, X.Y. Fang, W.D. Cook, G.A. Thouas, Q.Z. Chen, In vitro enzymatic degradation of poly (glycerol sebacate)-based materials, Biomaterials 32 (33) (2011) 8486–8496, https://doi.org/10.1016/j.biomaterials.2011.07.080.
[21] N.M. Krook, C. LeBlon, S.S. Jedlicka, In vitro examination of poly (glycerol sebacate) degradation kinetics: effects of porosity and cure temperature, MRS Online Proc. Libr. 1621 (2014) 87–92, https://doi.org/10.1557/opl.2014.68.
[22] S. Salehi, M. Fathi, S.H. Javanmard, T. Bahners, J.S. Gutmann, S. Ergün, T.A. Fuchsluger, Generation of PGS/PCL blend nanofibrous scaffolds mimicking corneal stroma structure, Macromol. Mater. Eng. 299 (4) (2014) 455–469, https://doi.org/10.1002/mame.201300187.
[23] A.P. Schuetze, W. Lewis, C. Brown, W.J. Geerts, A laboratory on the four-point probe technique, Am. J. Phys. 72 (2) (2004) 149–153, https://doi.org/10.1119/1.1629085.
[24] D. Gerlier, N. Thomasset, Use of MTT colorimetric assay to measure cell activation, J. Immunol. Methods 94 (1–2) (1986) 57–63, https://doi.org/10.1016/0022-1759(86)90215-2.
[25] P. Heydari, J. Varshosaz, M. Kharaziha, S.H. Javanmard, Antibacterial and pH-sensitive methacrylate poly-L-Arginine/poly (β-amino ester) polymer for soft tissue engineering, J. Mater. Sci. Mater. Med. 34 (4) (2023) 16, https://doi.org/10.1007/s10856-023-06720-8.
[26] B. Azimi, P. Nourpanah, M. Rabiee, S. Arbab, Poly (ϵ-caprolactone) fiber: an overview, Journal of Engineered Fibers and Fabrics 9 (3) (2014) 155892501400900309, https://doi.org/10.1177/155892501400900309.
[27] A. Fakhrali, M. Nasari, N. Poursharifi, D. Semnani, H. Salehi, M. Ghane, S. Mohammadi, Biocompatible graphene-embedded PCL/PGS-based nanofibrous scaffolds: a potential application for cardiac tissue regeneration, J. Appl. Polym. Sci. 138 (40) (2021) 51177, https://doi.org/10.1002/app.51177.
[28] A. Thakur, S. Kumar, V.S. Rangra, Synthesis of reduced graphene oxide (rGO) via chemical reduction, in: AIP Conference Proceedings, vol. 1661, AIP Publishing, 2015, May, https://doi.org/10.1063/1.4915423, 1.
[29] I. Yimlamai, S. Niamlang, P. Chanthaanont, R. Kunanuraksapong, S. Changkhamchom, A. Sirivat, Electrical conductivity response and sensitivity of ZSM-5, Y, and mordenite zeolites towards ethanol vapor, Ionics 17 (2011) 607–615, https://doi.org/10.1007/s11581-011-0545-3.
[30] R.A. Surmenev, A.N. Ivanov, A. Cecilia, T. Baumbach, R.V. Chernozem, S. Mathur, M.A. Surmeneva, Electrospun composites of poly-3-hydroxybutyrate reinforced with conductive fillers for in vivo bone regeneration, Open Ceramics 9 (2022) 100237, https://doi.org/10.1016/j.oceram.2022.100237.

[31] S. Sant, D. Iyer, A.K. Gaharwar, A. Patel, A. Khademhosseini, Effect of biodegradation and de novo matrix synthesis on the mechanical properties of valvular interstitial cell-seeded polyglycerol sebacate–polycaprolactone scaffolds, Acta Biomater. 9 (4) (2013) 5963–5973, https://doi.org/10.1016/j.actbio.2012.11.014.
[32] Z.J. Sun, L. Wu, W. Huang, X.L. Zhang, X.L. Lu, Y.F. Zheng, D.L. Dong, The influence of lactic on the properties of poly (glycerol–sebacate–lactic acid), Mater. Sci. Eng. C 29 (1) (2009) 178–182, https://doi.org/10.1016/j.msec.2008.06.010.
[33] N. Baheiraei, H. Yeganeh, J. Ai, R. Gharibi, M. Azami, F. Faghihi, Synthesis, characterization and antioxidant activity of a novel electroactive and biodegradable polyurethane for cardiac tissue engineering application, Mater. Sci. Eng. C 44 (2014) 24–37, https://doi.org/10.1016/j.msec.2014.07.061.
[34] D.E. Muylaert, J.O. Fledderus, C.V. Bouten, P.Y. Dankers, M.C. Verhaar, Combining tissue repair and tissue engineering; bioactivating implantable cell-free vascular scaffolds, Heart 100 (23) (2014) 1825–1830, https://doi.org/10.1136/heartjnl-2014-306092.
[35] R. Ravichandran, J.R. Venugopal, S. Sundarrajan, S. Mukherjee, S. Ramakrishna, Cardiogenic differentiation of mesenchymal stem cells on elastomeric poly (glycerol sebacate)/collagen core/shell fibers, World J. Cardiol. 5 (3) (2013) 28, https://doi.org/10.4330/wjc.v5.i3.28.
[36] K.K. Sadasivuni, D. Ponnamma, J. Kim, S. Thomas (Eds.), Graphene-based Polymer Nanocomposites in Electronics, Springer, Switzerland, 2015, pp. 1–382, https://doi.org/10.1007/978-3-319-13875-6.
[37] Y. He, H. Hou, S. Wang, R. Lin, L. Wang, L. Yu, X. Qiu, From waste of marine culture to natural patch in cardiac tissue engineering, Bioact. Mater. 6 (7) (2021) 2000–2010, https://doi.org/10.1016/j.bioactmat.2020.12.011.
[38] C.A. Sundback, J.Y. Shyu, Y. Wang, W.C. Faquin, R.S. Langer, J.P. Vacanti, T.A. Hadlock, Biocompatibility analysis of poly (glycerol sebacate) as a nerve guide material, Biomaterials 26 (27) (2005) 5454–5464, https://doi.org/10.1016/j.biomaterials.2005.02.004.
[39] K. Wang, M. Zhu, T. Li, W. Zheng, L.L. Xu, Q. Zhao, L. Wang, Improvement of cell infiltration in electrospun polycaprolactone scaffolds for the construction of vascular grafts, J. Biomed. Nanotechnol. 10 (8) (2014) 1588–1598, https://doi.org/10.1166/jbn.2014.1849.
[40] S. Salehi, T. Bahners, J.S. Gutmann, S.L. Gao, E. Mäder, T.A. Fuchsluger, Characterization of structural, mechanical and nano-mechanical properties of electrospun PGS/PCL fibers, Rsc Advances 4 (33) (2014) 16951–16957, https://doi.org/10.1039/C4RA01237B.
[41] P. Kerativitayanan, A.K. Gaharwar, Elastomeric and mechanically stiff nanocomposites from poly (glycerol sebacate) and bioactive nanosilicates, Acta Biomater. 26 (2015) 34–44, https://doi.org/10.1016/j.actbio.2015.08.025.
[42] M.A. Schroeder, P. Swietach, H.J. Atherton, F.A. Gallagher, P. Lee, G.K. Radda, D.J. Tyler, Measuring intracellular pH in the heart using hyperpolarized carbon dioxide and bicarbonate: a 13C and 31P magnetic resonance spectroscopy study, Cardiovasc. Res. 86 (1) (2010) 82–91, https://doi.org/10.1093/cvr/cvp396.
[43] Q. Chen, X. Yang, Y. Li, A comparative study on in vitro enzymatic degradation of poly (glycerol sebacate) and poly (xylitol sebacate), RSC Adv. 2 (10) (2012) 4125–4134, https://doi.org/10.1039/c2ra20113e.
[44] A.T. Habte, D.W. Ayele, Synthesis and characterization of reduced graphene oxide (rGO) started from graphene oxide (GO) using the tour method with different parameters, Adv. Mater. Sci. Eng. 2019 (2019), https://doi.org/10.1155/2019/5058163.